Boletim da Sociedade Astronômica Brasileira, **36**, no. 1, 122-125

3D simulations of the Tayler-Spruit dynamo in protoneutron stars

Resende, K. L. A.[1], Guerrero, G. A.[1], & Yokomizo, N. O.[1]

[1] Universidade Federal de Minas Gerais
e-mail: kevinresende_011@hotmail.com, guerrero@fisica.ufmg.br, yokomizo@fisica.ufmg.br

Abstract. Magnetars represent a special class of neutron stars (NS), characterized by slow rotation and the strongest magnetic fields observed in the universe, with surface field strengths ranging from 10^{14} G to 10^{15} G. Recently, it has been proposed that the magnetic field of a magnetar can be amplified through the Tayler-Spruit dynamo mechanism. In this scenario, part of the supernova remnant mass that gave rise to the neutron star is accreted onto its surface due to gravitational attraction, creating a shear layer. The poloidal field lines are wound up by differential rotation, predominantly resulting in toroidal fields, which are unstable to the Tayler Instability (TI). The instability induces the formation of non-axisymmetric poloidal fields, which are subsequently reorganized by differential rotation, regenerating the toroidal field and completing the dynamo loop. Barrère et al. (2023) investigated this process by simulating a proto-neutron star, modeling it as a spherically stratified and stable Couette flow, using the Boussinesq approximation of Magnetohydrodynamics (MHD), which assumes constant density, and identifying the presence of dynamos driven by the TI, which amplify the magnetic field to the magnitudes required for the formation of a magnetar. The present study aims to reproduce these simulation results using the EULAG-MHD code and to enhance the model by incorporating effects of General Relativity (GR). In this initial study, we introduce a relativistic correction to the local gravitational acceleration and employed a simple equation of state (EoS), described by a polytrope, to numerically solve the Tolman-Oppenheimer-Volkoff (TOV) equation of stellar structure in GR in order to obtain a non-uniform radial density profile that is more consistent with results derived from realistic EoS. We will present the thermodynamic profiles obtained from the TOV equation in the regime of hydrostatic equilibrium within the framework of GR.

Resumo. Os magnetares constituem uma classe especial de estrelas de nêutrons (NS), caracterizados por sua baixa rotação e pelos campos magnéticos mais intensos observados no universo, com magnitudes da ordem de 10^{14} G a 10^{15} G na superfície. Recentemente, foi proposto que o campo de um magnetar pode ser amplificado através do dínamo de Tayler-Spruit. Nesse cenário, parte da massa remanescente da supernova que deu origem à estrela de nêutrons é acretada em sua superfície devido à atração gravitacional, gerando uma camada de cisalhamento. As linhas de campo poloidal são distorcidas pela rotação diferencial, resultando predominantemente em campos toroidais, os quais são instáveis à Instabilidade de Tayler (TI). A instabilidade induz a formação de campos poloidais não axissimétricos, que são posteriormente reorganizados pela rotação diferencial, regenerando o campo toroidal e completando o ciclo do dínamo. Barrère et al. (2023) investigaram esse processo simulando uma protoestrela de nêutrons, modelando-a como um fluxo de Couette esfericamente estratificado e estável, utilizando a aproximação Boussinesq da Magnetohidrodinâmica (MHD) que assume densidade constante, e identificaram a presença de dínamos devido à TI, que amplificam o campo até a ordem necessária para a formação de um magnetar. O presente estudo visa reproduzir os resultados dessas simulações com o código EULAG-MHD e aprimorar o modelo incluindo efeitos da Relatividade Geral (GR). Neste primeiro estudo, introduzimos uma correção relativística na aceleração gravitacional local e empregamos uma equação de estado (EoS) simples, descrita por uma politropa, para resolver numericamente a equação de estrutura Tolman-Oppenheimer-Volkoff (TOV) da GR, a fim de obter um perfil radial de densidade não uniforme que seja mais compatível com resultados derivados de EoS realistas. Apresentaremos os perfis termodinâmicos obtidos pela equação TOV no regime de equilíbrio hidrostático no âmbito da GR.

Keywords. Magnetohydrodynamics (MHD) – Stars: magnetars – Dynamo

1. Introduction

Neutron Stars (NS), born in type II supernova explosions, are the final stage of the evolution of massive stars. They are one of the densest objects in the universe and exhibit strong magnetic fields with typical amplitudes ranging from 10^8 G to 10^{13} G.

Magnetars are a class of Neutron Stars characterized by their slow rotation and ultra-strong magnetic fields, being the most powerful magnets observed in the cosmos. According to spin-down measurements, it's estimated that a magnetar's dipole magnetic field can reach up to 10^{15} G on the surface (Olausen & Kaspi 2014). Historically, the magnetars were initially identified as two different objects, the Anomalous X-ray Pulsars (AXP) and Soft Gamma Repeaters (SGR), due to their emission of X-rays and soft γ rays, powered by the ultra-strong magnetic field activity, this is why Duncan & Thompson (1992) named these objects magnetars.

The origin of this extremely high magnetic field is uncertain. Ferrario & Wickramasinghe (2006) explored the fossil field hypothesis, in which the field is amplified by magnetic flux conservation during the collapse of the progenitor star. Although this scenario could explain such a high magnetic field, this would imply an initial field of order 10^4 G to the progenitor star, but, as mentioned by Spruit (2008), the rate of main sequence stars with such a large magnetic field is low, and does not match the fraction $0.4^{+0.6}_{-0.28}$ of NS being born as magnetars (Beniamini et al. 2019), which indicate that magnetars are likely as common as usual neutron stars.

A dynamo model is another explanation for this phenomenon, and it is a promising one. As proposed by Duncan & Thompson (1992), the field amplification might be due to the action of a dynamo, which is a continuous process that converts kinetic energy into magnetic energy. Most of the work published about magnetars' formation by dynamo action explores the possibility of convective dynamos or magnetorotational instability (MRI)-driven dynamos. Numerical simulation results indicate that both mechanisms improve their efficiency when the Protoneutron Star (PNS) is rotating fast (Raynaud et al. 2020; Reboul-Salze et al. 2021a).

All the possibilities mentioned above require the progenitor's core to be either highly magnetized or fast-rotating. Recently, Barrère et al. (2022) proposed a new scenario, where a magnetar's field could be generated in a PNS with a low rotation rate. This hypothesis suggests that when the supernova explodes, part of the mass ejected falls back into the PNS due to gravitational bond. Numerical simulations have shown that the accretion of mass, as it is asymmetric, may transfer sufficient angular momentum to spin up an NS, formed from a non-rotating $12M_\odot$ progenitor, to milliseconds periods (Chan, Müller & Heger 2020). In this scenario, the PNS's surface rotates faster than its interior, generating a positive shear. The differential rotation makes it possible to produce another type of dynamo, the Tayler-Spruit dynamo, first proposed by Spruit (2002), driven by radial shear and by the Tayler Instability (TI) (Tayler 1973).

In the Tayler-Spruit dynamo process, the axisymmetric poloidal field lines are wound up by differential rotation, leaving only the axisymmetric toroidal component, which is unstable to the TI. The instability generates non-axisymmetric poloidal components, which are reorganized by differential rotation to regenerate the toroidal field and close the dynamo loop. The proposed Tayler-Spruit dynamo received criticism from several authors (Denissenkov & Pinsonneault 2007; Zahn, Brun, & Mathis 2007). Fuller, Piro, & Jermyn (2019) revised the Tayler-Spruit dynamo, approaching the issue that non-axisymmetric poloidal fields cannot create an axisymmetric toroidal field, as pointed out by Zahn, Brun, & Mathis (2007), and demonstrated that an axisymmetric field could be created if non-linear terms are considered in the induction equation of the magnetic field. Monteiro et al. (2023) found that the TI is able to generate axisymmetric helicities capable to work as an α-effect.

The existence of the Tayler-Spruit dynamo has been discussed for a long time. Still, recently, Petitdemange, Marcotte, & Gissinger (2023, 2024); Daniel, Petitdemange, & Gissinger (2023) performed 3D numerical simulations of dynamo action in stably stratified Couette flow in the context of radiative layers, therefore, with negative shear, and observed characteristics similar to the theoretical Tayler-Spruit dynamo, following the scaling laws in agreement with Spruit (2002). Barrère et al. (2023) performed similar 3D numerical simulations but with positive shear, which is of interest to the new magnetar formation scenario proposed by the same authors, and successfully obtained amplification of the field to values compatible with the observations.

Barrère et al. (2023) approaches the problem by using the Boussinesq approximation of magnetohydrodynamics (MHD), which implies constant density, in addition to using Newtonian gravity for such a compact object. The present work aims to verify the validity of this approximation by computing the structure of a $1.4M_\odot$ neutron star considering a realistic equation of state applied to General Relativity (GR) and realistic gravitational acceleration. Stratification may be a crucial parameter in the model since it may affect the growth rate of the TI (Guerrero et al. 2019).

2. Structure Model

To obtain the structure model for our PNS, we use a spherically symmetric metric of the form:

$$ds^2 = -e^{2\Phi(r)/c^2}c^2dt^2 + e^{2\Psi(r)}dr^2 + r^2(d\theta^2 + sin^2\theta\, d\phi^2), \quad (1)$$

where $(x^\mu) = (ct, r, \theta, \phi)$ are spherical coordinates, and Φ and Ψ are radius-dependent functions that have yet to be determined by solving Einstein field equations:

$$G_{\mu\nu} = \frac{8\pi G}{c^4}T_{\mu\nu}, \quad (2)$$

which relates the components of the Einstein tensor, $G_{\mu\nu}$ (associated with the metric $g_{\mu\nu}$ and therefore with spacetime), with the components of the energy-momentum-stress tensor, $T_{\mu\nu}$ (associated with matter). G and c are, respectively, Newton's gravitational constant and the speed of light. For an observer comoving with the fluid (in its proper reference frame), we can write $T_{\mu\nu} = diag(\rho c^2, p, p, p)$, where ρ is the mass density and p the pressure, both measured in the rest frame of the fluid. Eq. 2 gives us a set of three differential equations,

$$\frac{1}{r^2}\frac{d}{dr}[r(1 - e^{-2\Psi})] = \frac{8\pi G}{c^2}\rho, \quad (3)$$

$$e^{-2\Psi}\left(\frac{2\Phi'}{c^2 r} + \frac{1}{r^2}\right) - \frac{1}{r^2} = \frac{8\pi G}{c^4}p, \quad (4)$$

$$e^{-2\Psi}\left[\frac{\Phi''}{c^2} + \left(\frac{\Phi'}{c^2} + \frac{1}{r}\right)\left(\frac{\Phi'}{c^2} - \Psi'\right)\right] = \frac{8\pi G}{c^4}p. \quad (5)$$

Here, the prime denotes a derivative with respect to r. Integrating Eq. 3, we find,

$$e^{-2\Psi} = 1 - \frac{2Gm(r)}{c^2 r}, \quad (6)$$

where

$$m(r) = \int_0^r \rho(r')\, 4\pi r'^2 dr'. \quad (7)$$

Finally, Eq. 4 and 5 give us,

$$\frac{dp}{dr} = -\frac{Gm\rho}{r^2}\left[1 + \frac{p}{\rho c^2}\right]\left[1 + \frac{4\pi r^3 p}{mc^2}\right]\left[1 - \frac{2Gm}{c^2 r}\right]^{-1}, \quad (8)$$

and

$$\frac{d\Phi}{dr} = -\left[\rho + \frac{p}{c^2}\right]^{-1}\frac{dp}{dr}, \quad (9)$$

where m, p and ρ are functions of r. Eq. 8 is known as the Tolman-Oppenheimer-Volkoff (TOV) equation, representing the hydrostatic equilibrium between pressure and gravity. In order to solve these coupled differential equations, we need an Equation of State (EoS) for the neutron star, which remains unknown to this day, especially near the center. There exist many realistic models of EoS[1], based on nuclear interactions and particle physics, but the one that best represents the NS's interior is still uncertain. Therefore, in this work, we will use a simplification and choose an EoS that mimics the general characteristics of these more sophisticated ones by writing a polytrope that relates pressure and density in the form:

$$p = K\rho^\gamma = K\rho^{1+1/n}. \quad (10)$$

We solve equations 7, 8 and 10 numerically, using as boundary conditions null surface density and central density of $\rho_c = 3\rho_0$, according to calculations by Benhar, Lovato, & Camelio (2022) for a $1.4M_\odot$ NS, where $\rho_0 = 0.16$ fm^{-3} is the equilibrium

[1] https://compose.obspm.fr/home/

density of Symmetric Nuclear Matter (SNM). The value of the constants K and n were chosen so that the NS would achieve simultaneously a mass of $1.4M_\odot$ and a radius in agreement with the ones obtained by the analyses of recent astrophysical data, i.e., 12.45 ± 0.65 km (Miller et al. 2021), $12.33^{+0.76}_{-0.81}$ km (Riley et al. 2019), $12.18^{+0.56}_{-0.79}$ km (Raaijmakers et al. 2021). With the values $n = 0.7$ ($\gamma \approx 2.43$) and $K = 3.08 \cdot 10^{-10}$ Pa $\left(\mathrm{kg/m^3}\right)^{-\gamma}$, we obtain $R = 12.46$ km, see Fig. 1.

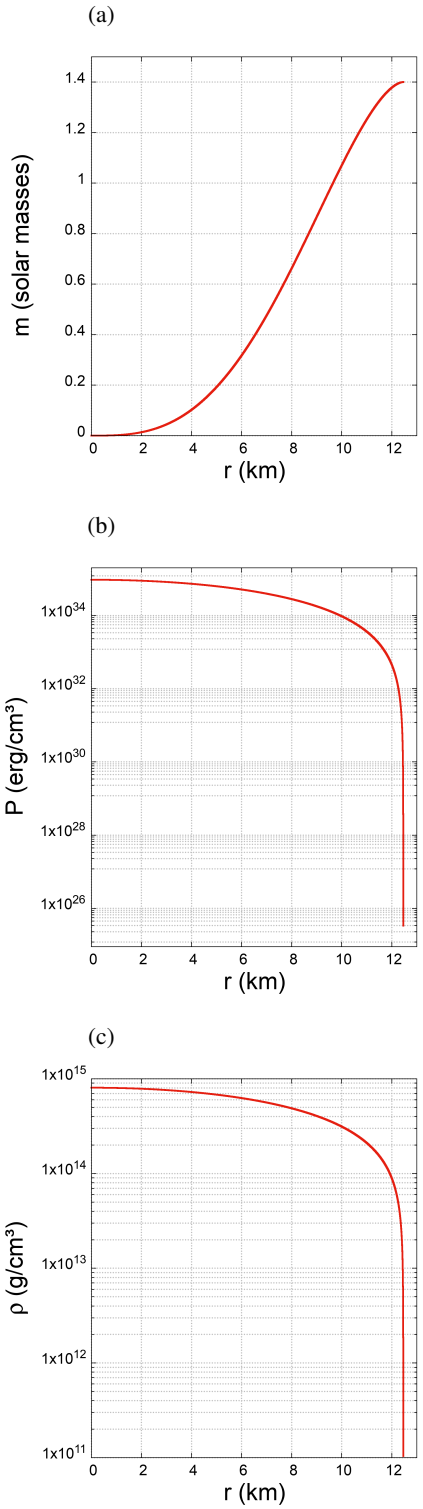

FIGURE 1: (a), (b) and (c) are, respectively, the mass, pressure and density profiles inside the neutron star.

The boundary conditions are fundamental to the model, as the choice of the central density changes the total mass and radius of the neutron star. In Fig. 2 we present M as a function of ρ_c and a diagram of M x R. In Fig 2a, we see that the maximum allowed mass for a NS in this model is $\approx 2.2M_\odot$, and also that in the regime we are interested ($M = 1.4M_\odot$), the model obeys the static stability criterion

$$\frac{dM}{d\rho_c} > 0. \tag{11}$$

Figure 2b relates the radius of the NS with its total mass for each value of ρ_c in Fig. 2a, and it shows that the model (red line) is consistent with the threshold of the black hole region (black line), since it remains on the right side of the black line.

An interested reader can compare some of our results with the ones obtained by more sophisticated EoS, for example, in Douchin & Haensel (2001). As mentioned before, besides the EoS, different choices of ρ_c lead to distinct models, but our model agrees in general with the profiles of Seif, Hashem & Abualhamd (2024), and, although we fitted our EoS specifically for a $1.4M_\odot$ based on observational data, Fig. 2a is in great agreement with the results of Shen et al. (1998).

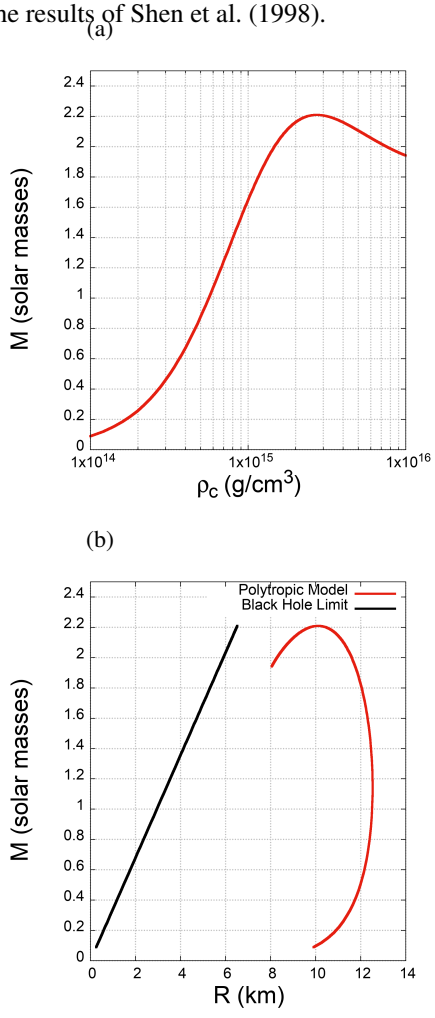

FIGURE 2: (a) Total mass as a function of central density. (b) Total mass and radius diagram. The red line represents our model and the black one separates the region of neutron stars (right) from the region of black holes (left).

Apart from a different thermodynamic profile, another relevant parameter for the TI is the gravitational field. Here we use

general relativity to describe the gravitational acceleration, g. Note that Eq. 8 is similar to the classical hydrostatic equilibrium with Newton's law of universal gravitation: $\frac{dP}{dr} = -\frac{Gm\rho}{r^2} = -g\rho$. In order to compare both equations, we need to change the radial coordinate of the TOV equation to a proper radial length, l, which are related, according to Eq. 1, by

$$dl = e^{\Psi(r)}dr. \tag{12}$$

Combining Eqs. 6 and 11, and substituting into Eq. 8, we obtain an expression compatible with quasi-Newtonian form $\frac{dP}{dl} = -g\rho$, from which we derive

$$g(r) = \frac{Gm}{r^2}\left(1 + \frac{P}{\rho c^2}\right)\left(1 + \frac{4\pi r^3 P}{mc^2}\right)\left(1 - \frac{2Gm}{rc^2}\right)^{-1/2}, \tag{13}$$

where we see the existence of three factors modifying the classical Newtonian acceleration, each of them approaches 1 in the non-relativistic limit.

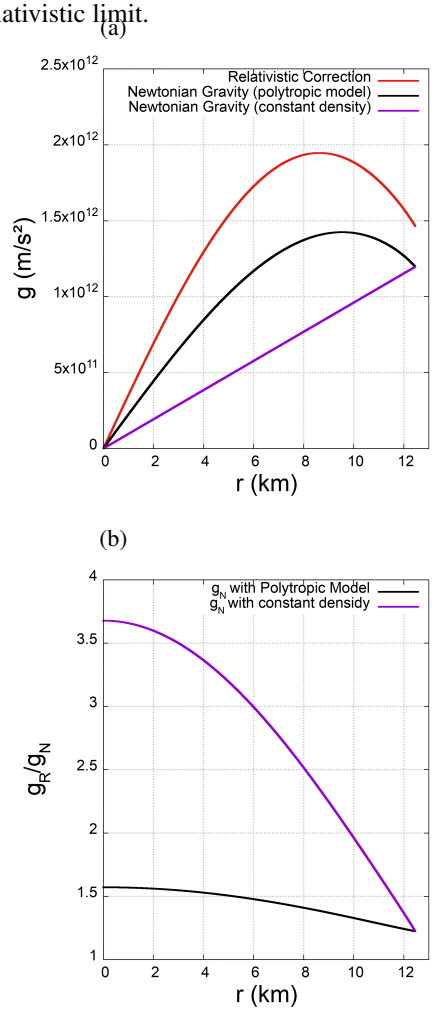

FIGURE 3: (a) Gravitational acceleration as a function of r inside the NS. Red: Relativistic correction using the polytropic model; Black: Newtonian gravity using our mass profile. Purple: Newtonian gravity with constant density profile. (b) Ratio between the relativistic gravity and the Newtonian gravity (each related by the same colors as in (a)).

Fig. 3 compares the values of this relativistic correction with two other cases of Newtonian gravity, one using our mass profile, from Fig. 1a, and another with constant density, as used by Barrère et al. (2023). It is known that gravity in GR is stronger than Newtonian gravity, and in this case, it's at least ~ 1.3 times stronger than the one used by Barrère et al. (2023), being able to achieve even ~ 3.5 near the center.

The effects of the density gradient and stronger gravity on the formation of magnetars via the Tayler-Spruit dynamo in 3D MHD simulations have not been studied yet and are our forthcoming endeavors.

3. Conclusion

In the present work, we proposed a structure model for a neutron star in hydrostatic equilibrium derived from general relativity and a polytropic equation of state, that agrees in general with the thermodynamic profiles of other models based on realistic equations of state. Also, we derived a realistic gravitational acceleration profile, which can be $\sim$ 30% (near the surface) to 250% (near the center) stronger than Newtonian gravity with constant density profile, as used by Barrère et al. (2023). Given that the structure is a well-established key factor for the Tayler instability (Guerrero et al. 2019), our forthcoming efforts are to insert our polytropic model into EULAG-MHD[2] code and investigate the effect of the density gradient, alongside with the stronger gravity profile.

Acknowledgements. This study was financed in part by the Coordenação de Aperfeiçoamento de Pessoal de Nível Superior – Brasil (CAPES) – Finance Code 001

References

Barrère, P., Guilet J., Reboul-Salze A., Raynaud R., & Janka H. T. 2022, A&A, 668, A79
Barrère, P., Guilet, J., Raynaud, R., & Reboul-Salze, A. 2023, MNRAS, 526, L88
Benhar, O., Lovato, A., & Camelio, G. 2022, ApJ 939 52
Beniamini, P., Hotokezaka, K., van der Horst, A., & Kouveliotou, C. 2019, MNRAS, 487, 1426
Chan, C., Müller, B., & Heger, A. 2020, MNRAS, 495, 3751
Daniel, F., Petitdemange, L., & Gissinger, C. 2023, Physical Review Fluids, 8, 123701
Denissenkov, P. A., & Pinsonneault, M. 2007, ApJ, 655, 1157
Douchin, F., & Haensel, P. 2001, A&A, 380, 151
Duncan, R. C., & Thompson, C. 1992, Astrophysical Journal Letters, 392, L9
Ferrario, L., & Wickramasinghe, D. 2006, MNRAS, 367, 1323
Fuller, J., Piro, A. L., & Jermyn, A. S. 2019, MNRAS, 485, 3661
Guerrero, G., Del Sordo, F., Bonanno, A., & Smolarkiewicz, P. K. 2019, MNRAS, 490, 4281
Miller, M. C. et al. 2021, ApJL, 918, L28
Monteiro, G., Guerrero, G., Del Sordo, F., Bonanno, A., & Smolarkiewicz, P. K. 2023, MNRAS, 521, 1415
Olausen, S. A., & and Kaspi, V. M. 2014, ApJS, 212, 6
Petitdemange, L., Marcotte, F., & Gissinger, C. 2023, Science, 379, 300
Petitdemange, L., Marcotte, F., Gissinger, C., & Daniel, F. 2024, A&A, 681, A75
Raaijmakers, G., Greif, S. K., Hebeler, K., Hinderer, T., Nissanke, S., Schwenk, A., Riley, T. E., Watts, A. L., Lattimer, J. M., & Ho, W. C. G. 2021, ApJL, 918, L29
Raynaud, R., Guilet, J., Janka, H.-T., & Gastine, T. 2020, Science Advances, 6, eaay2732
Reboul-Salze, A., Guilet, J., Raynaud, R., & Bugli, M. 2021a, A&A, 645, A109
Riley, T. E. et al. 2019, ApJL, 887, L21
Seif, W. M., Hashem, A. S., & Abualhamd, H. A. 2024 J. Phys. G: Nucl. Part. Phys., 51, 065203
Shen, H., Toki, H.,Oyamatsu, K., & Sumiyoshi, K. 1998, Nuclear Physics A, 637, 435
Smolarkiewicz, P. K. 2006, Int. J. Numer. Methods Fluids, 50, 1123
Spruit, H. C. 2002, A&A, 381, 923
Spruit, H.C. 2008, AIP Conference Proceedings, 983, 391
Tayler, R. J. 1973, MNRAS, 161, 365
Zahn, J. P., Brun, A. S., & Mathis, S. 2007, A&A, 474, 145

[2] https://www.astro.umontreal.ca/ paulchar/grps/eulag-mhd.html